# Nonlocal optics of plasmonic nanowire metamaterials

Brian M. Wells,[1] Anatoly V. Zayats,[2] and Viktor A. Podolskiy[1]
[1]*Department of Physics and Applied Physics, University of Massachusetts Lowell, Lowell, Massachusetts 01854, USA*
[2]*Department of Physics, King's College London, Strand, London WC2R 2LS, United Kingdom*
(Received 15 August 2013; revised manuscript received 16 December 2013; published 9 January 2014)

We present an analytical description of the nonlocal optical response of plasmonic nanowire metamaterials that enable negative refraction, subwavelength light manipulation, and emission lifetime engineering. We show that dispersion of optical waves propagating in nanowire media results from coupling of transverse and longitudinal electromagnetic modes supported by the nanowires and derive the nonlocal effective medium approximation for this dispersion. We derive the profiles of electric field across the unit cell, and use these expressions to solve the long-standing problem of additional boundary conditions in calculations of transmission and reflection of waves by nonlocal nanowire media. We verify our analytical results with numerical solutions of Maxwell's equations and discuss generalization of the developed formalism to other uniaxial metamaterials.

DOI: 10.1103/PhysRevB.89.035111 PACS number(s): 78.20.Ci, 42.70.−a, 78.20.Bh

## I. INTRODUCTION

Nanowire-based composites have recently attracted significant attention due to their unusual and counterintuitive optical properties that include negative refraction, subwavelength confinement of optical radiation, and modulation of photonic density of states [1–6]. Due to relatively low loss and ease of fabrication, nanowire composites found numerous applications in subwavelength imaging, biosensing, acousto-optics, and ultrafast all-optical processing, spanning visible to THz frequencies [7–19]. Wire materials are a subclass of uniaxial metamaterials that have homogeneous internal structure along one preselected direction. In all, this class of composites represents a flexible platform for engineering of optical landscape from all-dielectric birefringent media, to epsilon-near-zero, to hyperbolic, and epsilon-near-infinity regimes, each of which has its own class of benefits and applications [20–23].

In this work we present an analytical technique that provides adequate description of electromagnetism in wire-based metamaterials taking into account nonlocal optical response originating from the homogenization procedure. The approach can be straightforwardly extended to describe optics of coaxial-cable-like media [24–26] and numerous other uniaxial composites. The developed formalism reconciles the local and nonlocal effective-medium theories often used to describe the optics of nanowire composites in different limits [27–35]. More importantly, the formalism relates the origin of optical nonlocality to collective (averaged over many nanowires) plasmonic excitation of wire composite, and provides the recipe to implement additional boundary conditions in composite structures.

We illustrate the developed technique on the example of plasmonic nanowire metamaterials, formed by an array of aligned plasmonic nanowires embedded in a dielectric host. For simplicity, we fix the frequency of electromagnetic excitations and the unit cell parameters of the system, and vary only the permittivity of the wire inclusions. (The developed formalism can be readily applied for systems where both permittivity and frequency are changed at the same time.) We assume that the system operates in the effective-medium regime (its unit cell $a \ll \lambda_0$ with $\lambda_0$ being the free-space wavelength) and that the surface concentration of plasmonic wires is small $p = \pi R^2/a^2 \ll 1$. The parameters used in this work are $R = 20$ nm, $a = 100$ nm, $\epsilon_h = 1$ or $\epsilon_h = 2.25$, $L = 1$ $\mu$m, $\lambda_0 = 1.5$ $\mu$m (see Fig. 1), which are typical for composites fabricated with anodized alumina templates [2,13]. Supplementary information (SI) [36] presents the analysis of full-wave solutions of Maxwell equations in wire media.

## II. ELECTROMAGNETIC WAVES SUPPORTED BY BULK NANOWIRE COMPOSITES

As previously mentioned, the optical response of nanowire materials resembles that of uniaxial media with optical axis parallel to the direction of the nanowires ($z$). Therefore, dielectric permittivity tensor describing properties of waves propagating in the wire media is diagonal with components $\epsilon_x = \epsilon_y = \epsilon_{x,y}$ and $\epsilon_z$.

It has been shown that at optical and near-IR frequencies, the behavior of these components is largely described by Maxwell-Garnett type effective medium theory (EMT) [27–30,37]. In this approach, the microscopic distribution of the field is given by solutions of the Maxwell equations in quasistatic limit

$$\begin{aligned} E_z^{mg} &= \mathfrak{e}_z^{mg}, \\ E_x^{mg} &= \mathfrak{e}_x^{mg} \times \begin{cases} 2\frac{\epsilon_h}{\epsilon_h+\epsilon_i}, & r \leqslant R, \\ 1 + R^2 \frac{\epsilon_h-\epsilon_i}{\epsilon_h+\epsilon_i} \frac{y^2-x^2}{(x^2+y^2)^2}, & r > R, \end{cases} \end{aligned} \tag{1}$$

with $\epsilon_i$ and $\epsilon_h$ being the permittivities of wire inclusions and of host material, respectively, and parameters $\mathfrak{e}_x^{mg}$ and $\mathfrak{e}_z^{mg}$ are the field amplitudes. Straightforward averaging of the $j$th component ($j = x,y,z$) of the fields over the unit cell yields the effective permittivity $\epsilon_j^{mg} = \langle \epsilon(x,y) E_j^{mg}(x,y) \rangle / \langle E_j^{mg}(x,y) \rangle$:

$$\begin{aligned} \epsilon_{x,y}^{mg} &= \epsilon_h \frac{(1+p)\epsilon_i + (1-p)\epsilon_h}{(1+p)\epsilon_h + (1-p)\epsilon_i}, \\ \epsilon_z^{mg} &= p\epsilon_i + (1-p)\epsilon_h. \end{aligned} \tag{2}$$

By adjusting composition of the metamaterial and operating wavelength, the optical response of the composite can be controlled between all-dielectric elliptic ($\epsilon_{x,y}^{mg} > 0, \epsilon_z^{mg} > 0$),

 

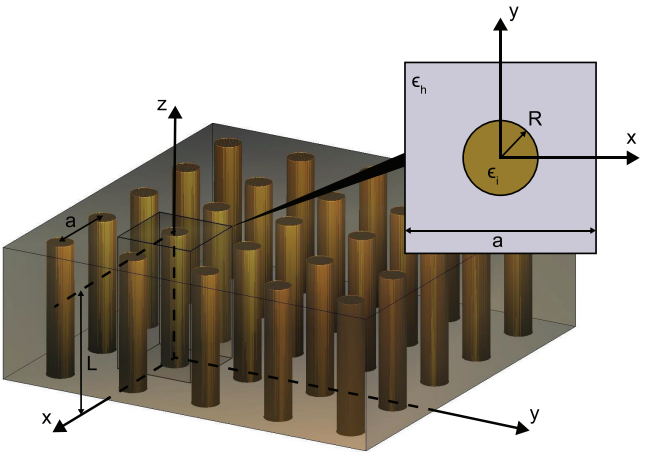


FIG. 1. (Color online) Schematic geometry and a unit cell of a nanowire composite.

epsilon-near-zero (ENZ, $\epsilon_z^{mg} \simeq 0$) and hyperbolic ($\epsilon_{x,y}^{mg} > 0, \epsilon_z^{mg} < 0$) regimes. In the two latter regimes, metamaterial supports optical waves with either small or large effective modal index motivating a number of potential applications in molding of light [20–22], cloaking [14–16], and subwavelength light manipulation [1,9–12].

At the same time, it has been shown that at lower frequencies where $-\epsilon_i \gg 1$, $\epsilon_z$ of wire composites becomes strongly nonlocal (exhibits strong dependence on $k_z$) [31–34]. Similar dependence has been recently shown to take place at visible frequencies in the ENZ regime [35]. Nonlocality, especially in the ENZ regime, has been shown to fundamentally alter the optical response of wire composite, leading to excitation of new types of optical waves, and requiring additional boundary conditions for analytical description of their excitation [32–35,38]. Despite extensive previous research, existing first-principal theoretical models describing optics of wire composites [32–34] cannot be used at visible and (near)-IR frequencies (see Appendix C), with remaining models requiring fitting [35] or numerical solutions of Maxwell equations. Here we present a formalism free of the above shortcomings.

The dispersion of plane waves propagating inside homogeneous (nonlocal) uniaxial materials can be derived from the well-known relation

$$\det\left|\vec{k}\cdot\vec{k}\,\delta_{ij} - k_i k_j - \epsilon_{ij}\frac{\omega^2}{c^2}\right| = 0, \tag{3}$$

with $\vec{k}$ and $\omega$ being the wave vector and the angular frequency of the plane wave, respectively, $c$ being the speed of light in vacuum, $\epsilon$ being the generally nonlocal dielectric permittivity tensor of the metamaterial, and subscripts $ij$ corresponding to Cartesian components [39]. In the local regime permittivity tensor is diagonal with $\epsilon_{ii} = \epsilon_i^{mg}$.

We now focus on the development of the model for the nonlocal effective permittivity of a nanowire composite. For propagation along the optical axis ($k_x = k_y = 0$), Eq. (3) allows two types of solutions. One is the well-known solution $k_z^{mg} = \sqrt{\epsilon_{x,y}}\omega/c$. In nanowire composites, this solution corresponds to the local permittivity $\epsilon_{xx} = \epsilon_{yy} = \epsilon_{x,y}^{mg}$ which is related to plasmonic oscillations perpendicular to the wire axes [27–30] and is thus influenced by the plasmonic resonance of the composite, slightly shifted from the position of the localized surface plasmon resonances in isolated wires due to interwire interaction.

The second solution of Eq. (3) corresponds to $\epsilon_z(k_z) = 0$. It describes a longitudinal wave propagating in the $z$ direction, with $\vec{E}\|\vec{k}\|\hat{z}$. This solution is also known as the additional (TM-polarized) wave.

As we show below, in nanowire systems this mode results from the interaction between cylindrical surface plasmon (CSP) modes [40] of the individual wires that comprise the collective (related to many wires) longitudinal electromagnetic mode. The components of the fields of the this mode can be related to its $z$ components that in turn can be written as a linear combination of cylindrical waves. For the square unit cell geometry, considered in this work, the latter combination will only contain cylindrical modes with $m = 0,4,8,\ldots$. Explicitly,

$$\begin{aligned} E_z^l &= e^{-ik_z^l z}\sum_m \cos(m\phi) \\ &\quad\times \begin{cases} a_m J_m(\kappa_i r), & r \leqslant R, \\ [\alpha_m^+ H_m^+(\kappa_h r) + \alpha_m^- H_m^-(\kappa_h r)], & r > R, \end{cases} \\ H_z^l &= e^{-ik_z^l z}\sum_m \begin{cases} 1, & m = 0 \\ \sin(m\phi), & m \geqslant 1 \end{cases} \\ &\quad\times \begin{cases} b_m J_m(\kappa_i r), & r \leqslant R, \\ [\beta_m^+ H_m^+(\kappa_h r) + \beta_m^- H_m^-(\kappa_h r)], & r > R, \end{cases} \end{aligned} \tag{4}$$

with $\kappa_{\{i,h\}}^2 + k_z^{l\,2} = \epsilon_{\{i,h\}}\omega^2/c^2$. Note that continuity of $E_z, H_z, E_\phi$, and $H_\phi$ at $r = R$ uniquely define the parameters $\alpha_m^+, \beta_m^+, a_m$, and $b_m$ as a function of $\alpha_m^-$, and $\beta_m^-$. The details of these derivations are provided in Appendix A.

The field of the mode has to satisfy the periodicity condition $E,H|_{x=-a/2} = E,H|_{x=+a/2}$. An analysis of the fields produced by a series in Eq. (4) suggests that such a solution can be realized when $\beta_m^- = 0$, and $k_z$ and $\alpha_m^-$ are obtained from the eigenvalue-type problem

$$\sum_m \widehat{\mathcal{H}}_{y\,jm}(k_z^l)\alpha_m^- = 0, \tag{5}$$

with $jm$ elements of matrix $\widehat{\mathcal{H}}_y$ corresponding to the $y$ component of the magnetic field produced by the $m_{\text{th}}$ Hankel function at the location $\{x,y\} = \{\frac{a}{2}, j\frac{a}{2N_m}\}$, with $N_m$ being the number of $m$ terms in Eq. (4) (see Appendix B for details). Our analysis suggests that as number of terms in Eq. (4) increases, the dispersion produced by this analytical technique quickly converges to the dispersion obtained by direct numerical solution of Maxwell's equations (here we use finite element method and rigorous-coupled-wave analysis [36]). Figure 2 demonstrates the excellent agreement between the numerical and analytical solutions corresponding to two- and three-term series $m = \{0,4\}$, $m = \{0,4,8\}$, and clearly demonstrates the longitudinal character of this mode. This wave is strongly dispersive in the regime $\epsilon_i \to -\epsilon_h$, corresponding to the surface plasmon oscillations on the metal-dielectric interface. On the other hand, when $-\epsilon_i \gg \epsilon_h$ (realized at mid-IR and lower frequencies for noble metals), the wave vector of the

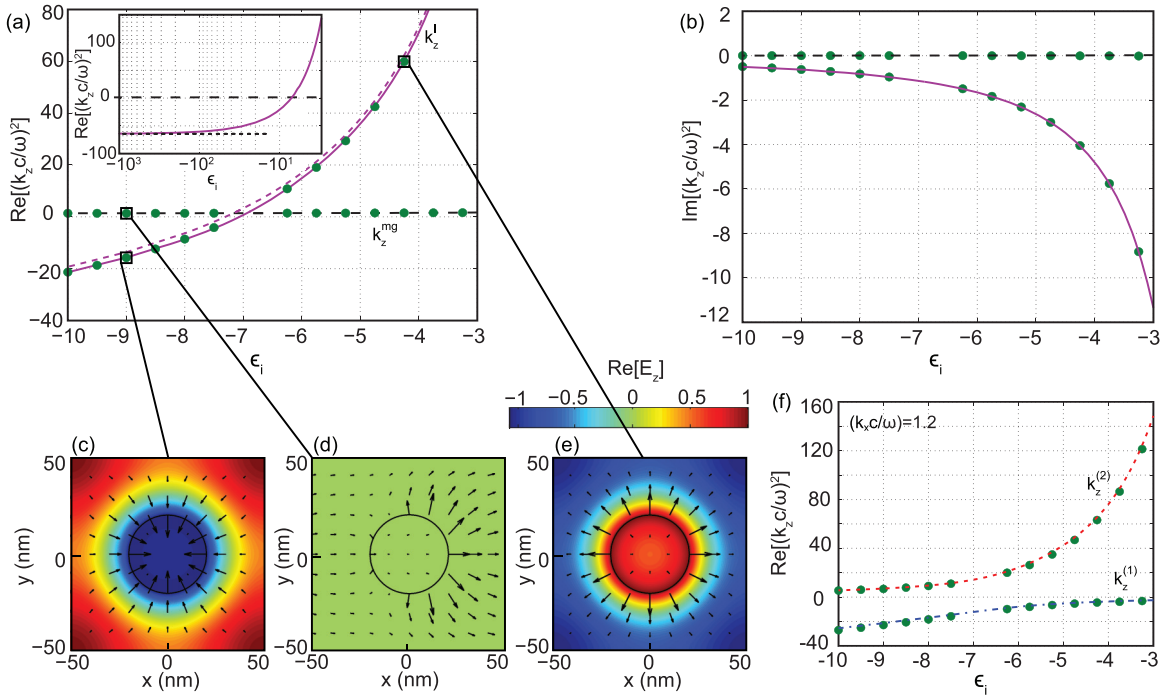


FIG. 2. (Color online) (a) and (b) Dispersion in nanowire composite ($\epsilon_h = 1$) as a function of wire permittivity. Dashed and solid lines represent transverse and longitudinal waves [$k_z^{mg}$ and $k_z^l$, Eq. (5), $m = \{0,4,8\}$], respectively; dotted line represents results of Eq. (5) for $m = \{0,4\}$; symbols represent numerical solutions of the Maxwell's equations; for $-\epsilon_i \gg \epsilon_h$, $k_z^l \to n_\infty^l \omega/c$ [dotted line in inset in (a)]. (c)–(e) electric field in the unit cell; surface plots and arrows represent $E_z$ and $\vec{E}_{x,y}$ components, respectively. (f) Modal dispersion for off-axis propagation [Eq. (7)].

longitudinal mode approaches $n_\infty^l \omega/c$, and its transverse counterpart approaches light line (see Refs. [32–34] and Fig. 2).

Comparing the dispersion relation corresponding to microscopic [Eq. (5)] and effective medium approximation $\epsilon_z(k_z) = 0$, a complete description of the nonlocal effective permittivity can be obtained. The functional dependence of nonlocal permittivity can be approximated as

$$\epsilon_z(k_z) = \xi\left(k_z^2 - k_z^{l\,2}\right)\frac{c^2}{\omega^2}, \tag{6}$$

where $k_z$ is the wave vector of the mode in the nonlocal effective medium approximation, $k_z^l$ is the wave vector of the mode of the composite in the microscopic theory, and $\xi$ is the factor which will be determined below.

The above considerations can be extended to the case of propagation of waves at an angle to the optical axis. For simplicity we consider the case $k_y = 0, k_x \neq 0$. It is relatively straightforward to transform Eq. (3) into a set of two uncoupled dispersion relations. For nanowire composites, the first of these, $k_x^2 + k_z^2 = \epsilon_{x,y}^{mg}\omega^2/c^2$ describes the propagation of transverse-electric (TE)-polarized waves. The second one, $\epsilon_z(k_z)(k_z^2 - \epsilon_{x,y}^{mg}\frac{\omega^2}{c^2}) = -\epsilon_{x,y}^{mg}k_x^2$, describes the propagation of the transverse-magnetic (TM)-polarized waves. Taking into account Eq. (6), the latter relation can be rewritten as

$$\left(k_z^2 - k_z^{l\,2}\right)\left(k_z^2 - \epsilon_{x,y}^{mg}\frac{\omega^2}{c^2}\right) = -\frac{\epsilon_{x,y}^{mg}}{\xi}\frac{\omega^2}{c^2}k_x^2 \tag{7}$$

that reflects the fact that similar to other nonlocal materials [38], nanowire composites support two TM-polarized waves propagating with different indices.

Equation (7) clearly shows that off-angle ($k_x \neq 0$) propagation of the two TM-polarized waves in anisotropic wire media can be mapped to a microscopic model of optical properties of a nanowire array. In this description, the two TM modes are determined by the components of the effective permittivities arising from (i) transverse (electron oscillations perpendicular to the nanowire axes) and (ii) longitudinal (electron oscillations and the wave vector parallel to the nanowire axes) parts of the cylindrical plasmons of the wires. The off-angle wave vector plays the role of the coupling constant. This nonlocality is present only in the effective medium model due to the homogenization procedure; in the microscopic model of the nanowire array, all the quantities are local.

The remaining free parameter of the model, multiplicative factor $\xi$, can be determined by requiring that in the limit of small $k_x$ the properties of one of the two TM-polarized waves follow elliptic or hyperbolic dispersion and has $k_z(k_x) =$ const dependence, observed in the wire media when $\epsilon_z^{mg} > 0$, $\epsilon_z^{mg} < 0$, and $\epsilon_z^{mg} \ll -1$, respectively [27–30,32–34]. The relationship

$$\xi = p\frac{\epsilon_i + \epsilon_h}{\epsilon_h - (n_\infty^l)^2} \tag{8}$$

adequately describes optics of wire media in these three limits. The excellent agreement between the predictions of Eq. (7) and the full-wave numerical solutions of Maxwell equations

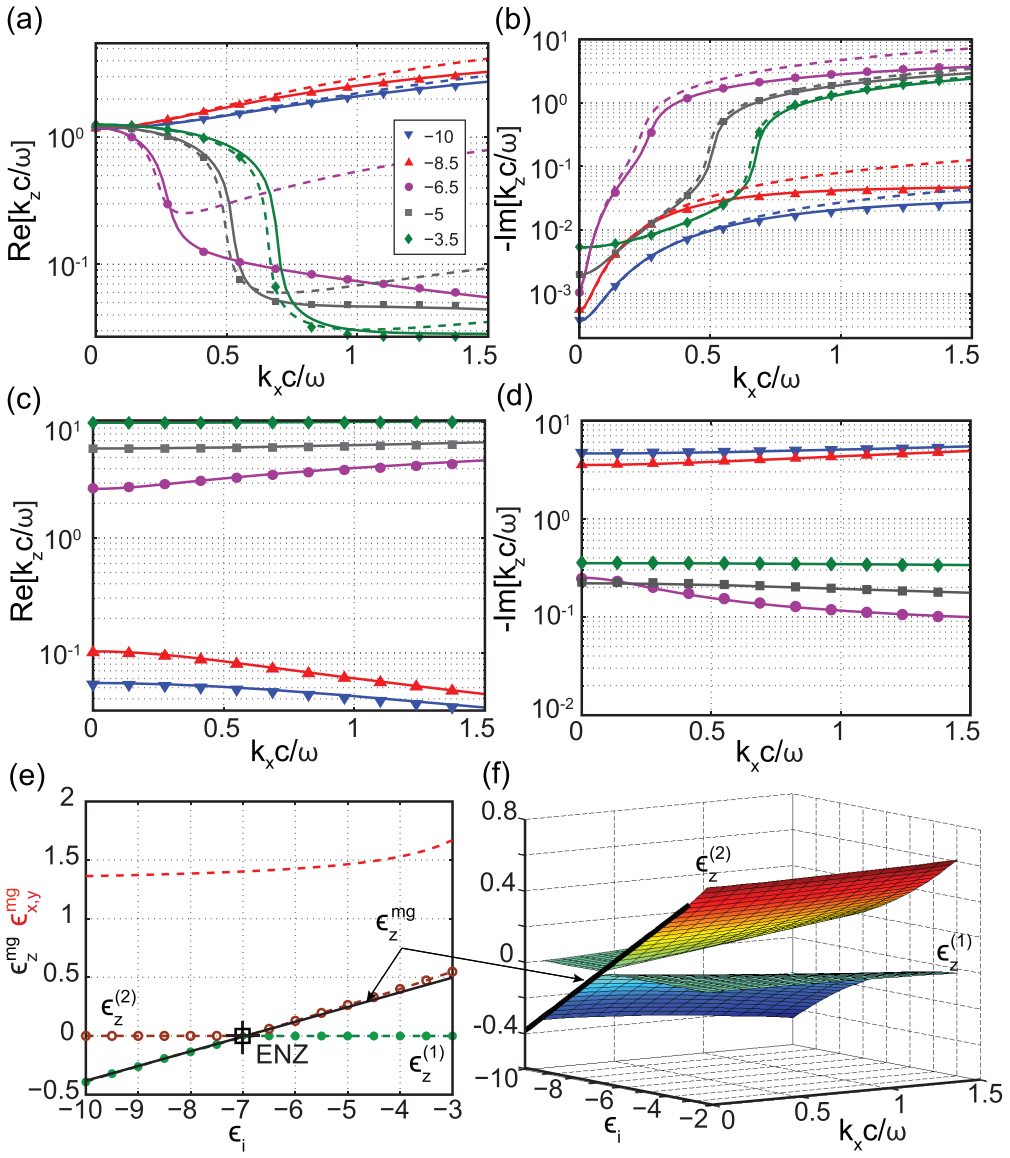


FIG. 3. (Color online) (a)–(d) Isofrequency contours of TM-polarized modes in nanowire composites with $\epsilon_h = 1$. Solid lines and symbols correspond to Eq. (7) and numerical solutions of Maxwell equations, respectively; dashed lines represent local EMT; (a) and (b) represent properties of main TM-polarized mode; (c) and (d) correspond to additional wave. (e) and (f) The effective medium permittivity of nonlocal nanowire composite for $k_x = 0$ (c) and for $k_x \neq 0$ (d); $\epsilon_z^{(1)}, \epsilon_z^{(2)}$ represent two solutions of Eq. (6); cross mark indicates ENZ condition ($\epsilon_z^{mg} \simeq 0$).

is shown in Figs. 2–4. As expected, the isofrequency of the "main" TM-polarized wave resembles ellipse or hyperbola that for small values of $k_x$ is well described by $\hat{\epsilon}^{mg}$. At the same time, the dependence $k_z(k_x)$ in "additional" wave is opposite to that of its main counterpart. The $z$ component of permittivity is described by Eq. (2) only for on-axis ($k_x = 0$) propagation, and exhibits strong spatial dispersion for oblique propagation of light.

The presented formalism provides a mechanism to calculate the deviation of the dispersion of the waves in nanowire materials from the prediction of local effective medium technique. In particular, this deviation places fundamental limits on subwavelengh light manipulation and on increase of local density of photonics states [3–6]. It is also likely to affect the cloaking performance of nanowire-based structures [14–16].

Now that the origin and dispersion of the modes propagating in nanowire systems is understood, we focus on the analysis of the optical properties of finite-size wire arrays. Since in the EMT approximation the fields of TE- and TM-polarized modes are orthogonal to each other, and since propagation of TE-polarized light through the wire-based system is only affected by $x, y$ components of permittivity, this propagation can be successfully described by Eq. (2) [27–30]. Here we focus on the analysis of propagation of TM-polarized light. This analysis must answer two important questions: (i) What is the structure of electromagnetic waves propagating in the system, and (ii) what are the additional boundary conditions needed to determine the amplitudes of the two TM-polarized modes inside the wire system?

Consistent effective medium description requires that the unit-cell averaged fields satisfy both constituent relations $\epsilon_j =$

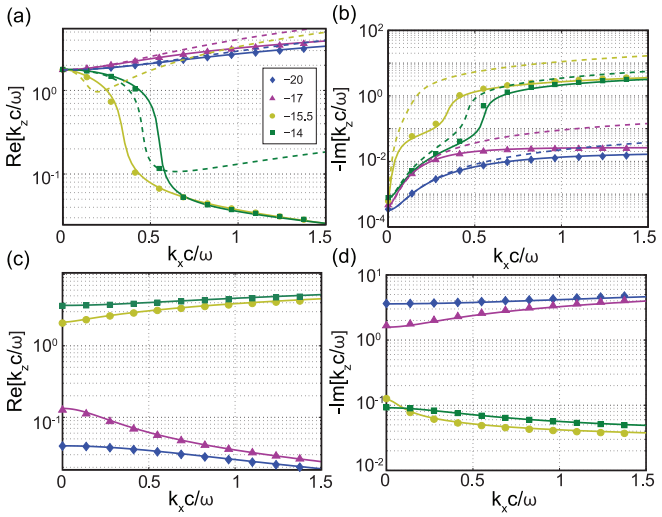


FIG. 4. (Color online) Same as Figs. 3(a)–3(d) for $\epsilon_h = 2.25$.

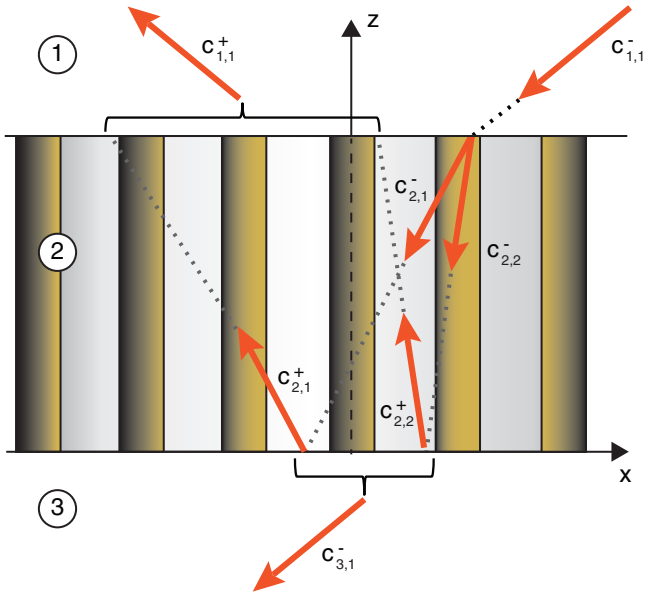


FIG. 5. (Color online) Schematic of TMM for a nanowire composite. Each mode is labeled to clarify notation as well as interface numbers.

$\langle \epsilon E_j \rangle / \langle E_j \rangle$ and relations between the field components of the plane wave $\langle \epsilon E_z \rangle = -k_x/k_z \langle \epsilon E_x \rangle$. With these constraints, we start from Eqs. (1) and (4), determine the parameters $\alpha_0^-, \epsilon_z^{mg}$, and $\epsilon_x^{mg}$ by normalizing $\langle E_z^l \rangle = \langle E_x^{mg} \rangle = \langle E_z^{mg} \rangle = 1$, and construct the fields of the two waves propagating in the wire media as $\vec{E}(x,y)e^{i\omega t - ik_x x - ik_z z}$ with

$$\begin{aligned} E_x(x,y) &= E_x^{mg}, \\ E_z(x,y) &= \gamma^{mg} E_z^{mg} + \gamma^l E_z^l|_{z=0}, \end{aligned} \tag{9}$$

and

$$\begin{aligned} \gamma^{mg} &= -\frac{\epsilon_{x,y}^{mg} k_x}{\epsilon_z k_z} \frac{\epsilon_z - \epsilon^l}{\epsilon_z^{mg} - \epsilon^l}, \\ \gamma^l &= -\frac{\epsilon_{x,y}^{mg} k_x}{\epsilon_z k_z} \frac{\epsilon_z - \epsilon_z^{mg}}{\epsilon^l - \epsilon_z^{mg}}. \end{aligned} \tag{10}$$

In the expressions above $\epsilon_z \equiv \epsilon_z(k_z)$ is given by Eq. (6), $k_z(k_x)$ by Eq. (7), and $\epsilon^l = \langle \epsilon(x,y) E_z^l(x,y) \rangle / \langle E_z^l(x,y) \rangle$.

Equation (9) represents a transition between full-wave solutions of Maxwell equations in the nanowire array where the fields oscillate on the scale of the individual wires, and effective-medium solutions where plane waves propagate in the homogenized material. Since our model for $\vec{E}^{mg}$ assumes quasistatic limit [Eq. (1)], Eq. (9) is technically valid in the limit $a \ll 2\pi/k_x, a \ll \lambda_0$. Any effective medium technique is expected to fail in the limit $k_x \gtrsim 2\pi/a$.

## III. TRANSMISSION AND REFLECTION PROPERTIES OF NONLOCAL METAMATERIAL SLABS

Finally, we consider the problem of reflection/refraction of light at the interface of nonlocal (meta-) materials, extending the well-developed transfer-matrix formalism [41,42] to nonlocal composites. The typical geometry of light propagation through a finite-thickness slab of nanowire material is shown in Fig. 5.The problem of calculating reflection/transmission of light through the slab of nanowire material can be reduced to the problem of finding the amplitudes of reflected and transmitted waves throughout the system in terms of the amplitude of the single wave incident on the material ($c_{1,1}^-$). This problem, in turn, can be reduced to the problem of finding the amplitudes of waves scattered by each individual interface in terms of the amplitudes of the (multiple) waves incident at this interface.

Maxwell equations require continuity of (microscopic) $E_x$ and $D_z$, and the effective-medium boundary conditions can be obtained by averaging these relationships across the unit cell. Multiple, linearly independent boundary conditions can be obtained by requiring the continuity of $\mathbb{E}^n = \langle e^{2\pi i n \frac{x}{a}} E_x \rangle$ and $\mathbb{D}^n = \langle e^{2\pi i n \frac{x}{a}} D_z \rangle$ with different integer $n$.

In particular, for the interface between two conventional materials, continuity of $\mathbb{E}^0, \mathbb{D}^0$ yield conventional TMM results. If one of the media is nonlocal metamaterial, we suggest to complement the above boundary conditions by the additional boundary condition (ABC) of continuity of $\mathbb{D}^1$ (if both materials are nonlocal, addition of second ABC of continuity of $\mathbb{E}^1$ is required). Explicitly, assuming that the top interface is located at $z = z_0$, the boundary conditions for this interface are implemented as

$$\begin{aligned} &c_{1,1}^+ \mathbb{E}_{1,1}^0 e^{ik_{z_{1,1}} z_0} + c_{1,1}^- \mathbb{E}_{1,1}^0 e^{-ik_{z_{1,1}} z_0} \\ &\quad = \sum_{l=1,2} c_{2,l}^+ \mathbb{E}_{2,l}^0 e^{ik_{z_{2,l}} z_0} + c_{2,l}^- \mathbb{E}_{2,l}^0 e^{-ik_{z_{2,l}} z_0}, \\ &c_{1,1}^+ \mathbb{D}_{1,1}^0 e^{ik_{z_{1,1}} z_0} - c_{1,1}^- \mathbb{D}_{1,1}^0 e^{-ik_{z_{1,1}} z_0} \\ &\quad = \sum_{l=1,2} c_{2,l}^+ \mathbb{D}_{2,l}^0 e^{ik_{z_{2,l}} z_0} - c_{2,l}^- \mathbb{D}_{2,l}^0 e^{-ik_{z_{2,l}} z_0}, \\ &c_{1,1}^+ \mathbb{D}_{1,1}^1 e^{ik_{z_{1,1}} z_0} - c_{1,1}^- \mathbb{D}_{1,1}^1 e^{-ik_{z_{1,1}} z_0} \\ &\quad = \sum_{l=1,2} c_{2,l}^+ \mathbb{D}_{2,l}^1 e^{ik_{z_{2,l}} z_0} - c_{2,l}^- \mathbb{D}_{2,l}^1 e^{-ik_{z_{2,l}} z_0}. \end{aligned} \tag{11}$$

In the expressions above the double subscript represents the layer number in the system and the mode number within

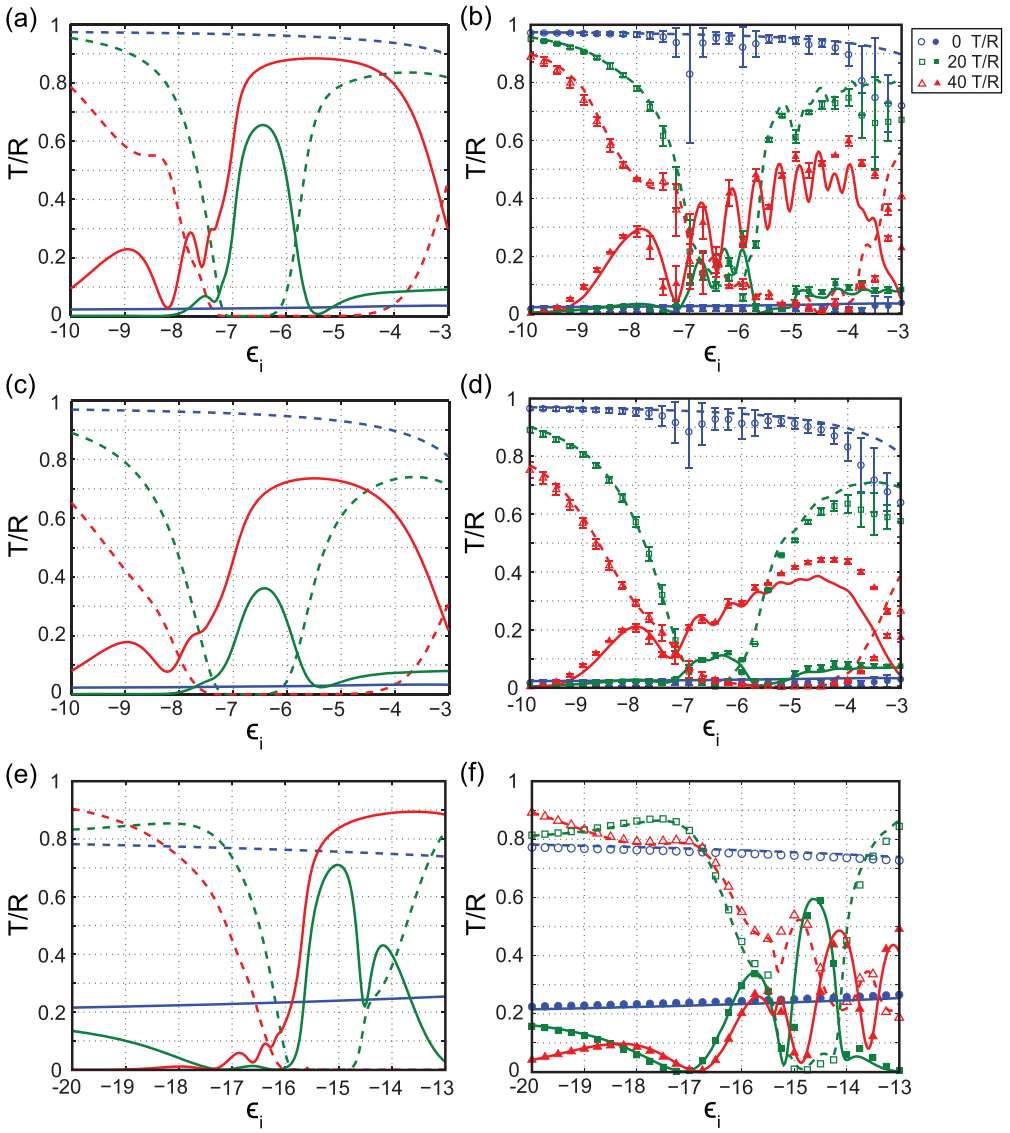


FIG. 6. (Color online) Transmission and reflection of light through a parallel slab of nanowire media, suspended in air for (a)–(d) and in polymer with $\epsilon_h = 2.25$ (e) and (f) with $\mathrm{Im}(\epsilon_i) = -0.1$ (a), (b), (e), and (f), and $\mathrm{Im}(\epsilon_i) = -0.25$ (c) and (d). (a), (c), and (e): Local TMM calculations. (b), (d), and (f): TMM simulations with the nonlocal EMT developed here (lines) and numerical solutions of Maxwell equations (symbols). Solid lines and filled symbols represent reflection. Dashed lines and empty symbols represent transmission; different colors/shapes correspond to different angles for incident angles, blue circles: 0°, green squares: 20°, red triangles: 40°.

the layer, while the "±" superscript represent the direction of the wave propagation (see Fig. 5). The amplitudes of the wave propagating in the system represent the amplitude of $\mathbb{E}^0$; therefore, the amplitudes of $E_x$ are symmetric with respect to change of propagation direction $k_z \to -k_z$, while the amplitudes of $E_z, D_z$ are antisymmetric

Note that since polarization along the optical axis $P_z$ is dominated by the field of longitudinal wave, this ABC is close to the heuristic condition $P_\perp^{\mathrm{nonlocal}} = 0$, proposed for homogeneous [38] and composite [35] materials, and to condition of continuity of $\epsilon_h \mathbb{E}^0$, suggested for ultrathin high-conductivity wires [32–34] (in general the above ABCs are not identical to each other). When both media across the interface are nonlocal, continuity of $\mathbb{E}^1$ plays the role of the second additional boundary condition. Note that due to presence of longitudinal modes on both sides of the interface, $P_\perp^{\mathrm{nonlocal}}$ may not vanish in this configuration. As an additional crosscheck, the proposed combination of ABCs ensures full transmission of light through "virtual" interface between two identical nanowire metamaterials.

Transmission and reflection of metamaterial are compared to the full-vectorial numerical solutions of Maxwell's equations, predictions of conventional (local) effective medium theory, and predictions of the nonlocal EMT developed in this work in Fig. 6. It is seen the smaller the loss and the larger the angle of incidence the more important it becomes to take into account the nonlocal optics of nanowire composites. Interestingly, nonlocal response strongly affects optical response of the wire metamaterials across the broad range of the effective permittivities. This effect is most clearly seen in reflection, but is also visible in transmission, especially in the ENZ regime.

## IV. CONCLUSIONS

We presented an approach to describe optics of nonlocal wire metamaterials across the whole optical spectrum. The formalism demonstrates excellent agreement with the results of numerical solutions of Maxwell's equations and is essential in development of an adequate description of optics in wire arrays, from understanding the true density of photonic states to the limits of resolution in these systems. Although not presented here, in our studies we also varied radius and lattice size in the composite (within $p \lesssim 0.3$ limit of applicability of Maxwell-Garnett formalism [29]), and obtained good agreement between analytical and numerical solutions of Maxwell equations. The developed formalism can be straightforwardly extended to describe the optics of other wirelike composites including coated wire structures, and coax-cable-based systems [24–26].

## ACKNOWLEDGMENTS

This research is supported by US Army Research Office (Grant No. W911NF-12-1-0533), EPSRC (UK), and the ERC iPLASMM project (321268).

## APPENDIX A: DISTRIBUTION OF ELECTROMAGNETIC FIELDS ACROSS THE UNIT CELL

Since the geometry of the system (see Fig. 1) is homogeneous along the $z$ direction, the field in the unit cell can be represented as a linear combination of cylindrical waves having a well-defined value of the wave vector component $k_z$, given by Eq. (4).

The symmetry of the unit cell chosen in our work dictates the choice of $m = 0,4,8,\ldots$. The approach can be generalized to different unit cells by choosing an appropriate combination of $m$ values. The technique can be further generalized by replacing $\{\sin m\phi, \cos m\phi\} \to \exp im\phi$ and expanding the summation over positive and negative values of $m$. In-plane components of the microscopic fields can be expressed as follows:

$$
\begin{aligned}
E_r^l &= \frac{i}{\kappa^2}\left(k_z^l \frac{\partial E_z^l}{\partial r} + \frac{\omega}{rc}\frac{\partial H_z^l}{\partial \phi}\right),\\
E_\phi^l &= \frac{i}{\kappa^2}\left(\frac{k_z^l}{r}\frac{\partial E_z^l}{\partial \phi} - \frac{\omega}{c}\frac{\partial H_z^l}{\partial r}\right),\\
H_r^l &= \frac{i}{\kappa^2}\left(-\frac{\epsilon\omega}{rc}\frac{\partial E_z^l}{\partial \phi} + k_z^l \frac{\partial H_z^l}{\partial r}\right),\\
H_\phi^l &= \frac{i}{\kappa^2}\left(\frac{\epsilon\omega}{c}\frac{\partial E_z^l}{\partial r} + \frac{k_z^l}{r}\frac{\partial H_z^l}{\partial \phi}\right).
\end{aligned}
\tag{A1}
$$

Equation (A1) is valid both inside ($r \leqslant R$) and in-between ($r > R$) the nanowires; the value of $r$ determines the choice of

$$
\epsilon,\kappa = \begin{cases} \epsilon_i,\kappa_i, & r \leqslant R,\\ \epsilon_h,\kappa_h, & r > R. \end{cases}
$$

For brevity, from this point on, we omit the arguments of Bessel functions; unless otherwise specified, it is assumed that $J_m = J_m(\kappa_i r)$; $H_m^{\pm} = H_m^{\pm}(\kappa_h r)$.

Note that only one of the three sets of coefficients $\{a_m,b_m\},\{\alpha_m^+,\beta_m^+\}$, and $\{\alpha_m^-,\beta_m^-\}$ is independent. We begin by using the continuity of the tangential components of the electric and magnetic fields at $r = R$ to obtain an expression for $\{a_m,b_m\},\{\alpha_m^+,\beta_m^+\}$ in terms of $\{\alpha_m^-,\beta_m^-\}$. Explicitly, the linear relationship

$$
\begin{pmatrix} \alpha_m^+ \\ \vdots \\ \beta_m^+ \end{pmatrix} = \hat{S} \begin{pmatrix} \alpha_m^- \\ \vdots \\ \beta_m^- \end{pmatrix} \tag{A2}
$$

can be derived from

$$
\begin{aligned}
&\begin{bmatrix} \frac{k_z^l m H_m^+}{R}\left(\frac{1}{\kappa_i^2} - \frac{1}{\kappa_h^2}\right) & \frac{\omega}{c}\left(\frac{J_m' H_m^+}{\kappa_i J_m} - \frac{H_m'^+}{\kappa_h}\right) \\ \frac{\omega}{c}\left(\frac{\epsilon_i J_m' H_m^+}{\kappa_i J_m} - \frac{\epsilon_h H_m'^+}{\kappa_h}\right) & \frac{k_z^l m H_m^+}{R}\left(\frac{1}{\kappa_i^2} - \frac{1}{\kappa_h^2}\right) \end{bmatrix} \begin{pmatrix} \alpha_m^+ \\ \beta_m^+ \end{pmatrix}\\
&= \begin{bmatrix} \frac{k_z^l m H_m^-}{R}\left(\frac{1}{\kappa_i^2} - \frac{1}{\kappa_h^2}\right) & \frac{\omega}{c}\left(\frac{J_m' H_m^-}{\kappa_i J_m} - \frac{H_m'^-}{\kappa_h}\right) \\ \frac{\omega}{c}\left(\frac{\epsilon_i J_m' H_m^-}{\kappa_i J_m} - \frac{\epsilon_h H_m'^-}{\kappa_h}\right) & \frac{k_z^l m}{R}\left(\frac{1}{\kappa_i^2} - \frac{1}{\kappa_h^2}\right) H_m^- \end{bmatrix} \begin{pmatrix} \alpha_m^- \\ \beta_m^- \end{pmatrix},
\end{aligned}
\tag{A3}
$$

where each of the four submatrices is a diagonal matrix with its elements corresponding to the Bessel function combinations evaluated at $r = R$. In this cylindrically symmetric case, the $S$ matrix can be formally divided into four (diagonal) submatrices

$$
\hat{S} = \begin{bmatrix} S_{11} & S_{12} \\ S_{21} & S_{22} \end{bmatrix}. \tag{A4}
$$

The components $S_{11}$ and $S_{22}$ represent polarization-preserving TE, TM reflection, while the components $S_{12},S_{21}$ represent polarization-mixing coupling of TM to TE waves. Note that in the cylindrical geometry, polarization-preserving reflection is only possible when either $m = 0$ or $k_z = 0$, which yields $\det S_{12} = \det S_{21} = 0$.

The relationships

$$
\begin{aligned}
a_m J_m &= \alpha_m^+ H_m^+ + \alpha_m^- H_m^-,\\
b_m J_m &= \beta_m^+ H_m^+ + \beta_m^- H_m^-
\end{aligned}
\tag{A5}
$$

allow one to calculate the amplitudes $\{a,b\}$ based on the amplitudes of $\{\alpha^-,\beta^-\}$.

Combined, Eqs. (1), (A1), (A2), (A3), and (A5) provide complete information about the field distribution inside the unit cell once the parameters $k_z^l$ and $\{\alpha^-,\beta^-\}$ are known. The formalism presented here can be straightforwardly expanded to calculate the field inside the structures with more complicated unit cells, that include multishelled wires, coax-cable-like systems, etc. (see, e.g., Refs. [24–26]). The formalism can be further extended to calculate fields inside the systems with noncircular cross section of the wires, in which case the $S$ matrix ceases to be block diagonal [43–45].

## APPENDIX B: DISPERSION OF THE LONGITUDINAL MODE

We now focus on the problem of calculating the dispersion of the mode, which reduces to the problem of calculating the relationship between internal structure of the unit cell and the set of parameters $k_z$ and $\{\alpha^-,\beta^-\}$. The field of the eigenmode propagating in the periodic array of wires should

satisfy the Bloch-periodicity condition

$$\left.\begin{matrix} E \\ H \end{matrix}\right|_{x=-\frac{a}{2},y} = \left.\begin{matrix} E \\ H \end{matrix}\right|_{x=+\frac{a}{2},y} \tag{B1}$$

(here we enforce periodicity of $y$ components of electric and magnetic fields). Although this condition should ideally be satisfied for all values of the $y$ coordinate from the interval $y \in [-a/2, a/2]$, in practice it suffices to enforce the Bloch-periodicity condition for a number of fixed points $\{x_j, y_j\}$ equal to the number of $m$ values in Eq. (4). In our calculations we assume $y_j = \frac{a}{2N_m} j$, with $N_m$ being the number of $m$ terms in expansion in Eq. (4). Our analysis suggests that the choice of the exact location of the points does not significantly alter the dispersion of the mode, derived with the technique described in this work.

Noting that $\sin(\phi) = \sin(\pi - \phi)$, $\cos(\phi) = -\cos(\pi - \phi)$, $\sin(m\phi) = -\sin[m(\pi - \phi)]$, and $\cos(m\phi) = \cos[m(\pi - \phi)]$, it can be shown that components of electric and magnetic field possess the following symmetry:

$$E_y(x,y) = E_y(-x,y),$$
$$H_y(x,y) = -H_y(-x,y).$$

Therefore, Eq. (B1) becomes equivalent to

$$\begin{pmatrix} \hat{0} & \hat{0} \\ \widehat{\widetilde{H}^+} & \widehat{H^+} \end{pmatrix} \begin{pmatrix} \alpha_m^+ \\ \beta_m^+ \end{pmatrix} + \begin{pmatrix} \hat{0} & \hat{0} \\ \widehat{\widetilde{H}^-} & \widehat{H^-} \end{pmatrix} \begin{pmatrix} \alpha_m^- \\ \beta_m^- \end{pmatrix} = \begin{pmatrix} 0 \\ 0 \end{pmatrix}, \tag{B2}$$

where the elements of the submatrices $H^{\pm}$ are evaluated based on Eqs. (1), (A1), and (A2) according to the following rules: The submatrices $\tilde{H}$ and $H$ represent the magnetic field of TM- and TE-polarized waves, respectively; the superscript of the expression $\pm$ corresponds to the superscript of the Hankel function; and the $jm_{\text{th}}$ element of each submatrix represent the $y$ component of the magnetic field due to $m_{\text{th}}$ Hankel function, evaluated at the point $\{x_j, y_j\} = \{a/2, y_j\}$.

With the help of the $S$ matrix, Eq. (B2) can be further simplified as

$$\begin{pmatrix} \hat{0} & \hat{0} \\ \widehat{\widetilde{H}^+}\widehat{S_{11}} + \widehat{H^+}\widehat{S_{21}} + \widehat{\widetilde{H}^-} & \widehat{\widetilde{H}^+}\widehat{S_{12}} + \widehat{H^+}\widehat{S_{22}} + \widehat{H^-} \end{pmatrix} \begin{pmatrix} \alpha_m^- \\ \beta_m^- \end{pmatrix} = \begin{pmatrix} 0 \\ 0 \end{pmatrix}. \tag{B3}$$

Finally, we represent the amplitudes of the field of longitudinal TM-polarized wave as $\binom{\alpha_m^-}{0}$ with values of the coefficients

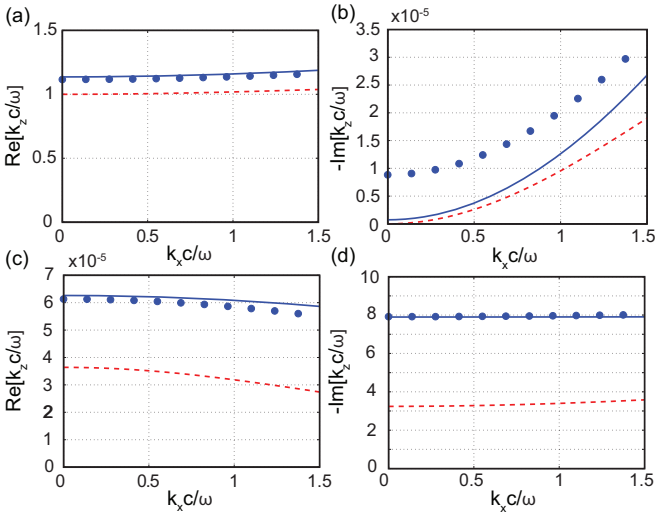


FIG. 8. (Color online) Same as Fig. 7 but for highly conductive wires $\epsilon_i = -200 - 0.1i$; note that $|\text{Im}[k_z c/\omega]| \ll |\text{Re}[k_z c/\omega]|$ in (a) and (b) and that $|\text{Im}[k_z c/\omega]| \gg |\text{Re}[k_z c/\omega]|$ in (c) and (d).

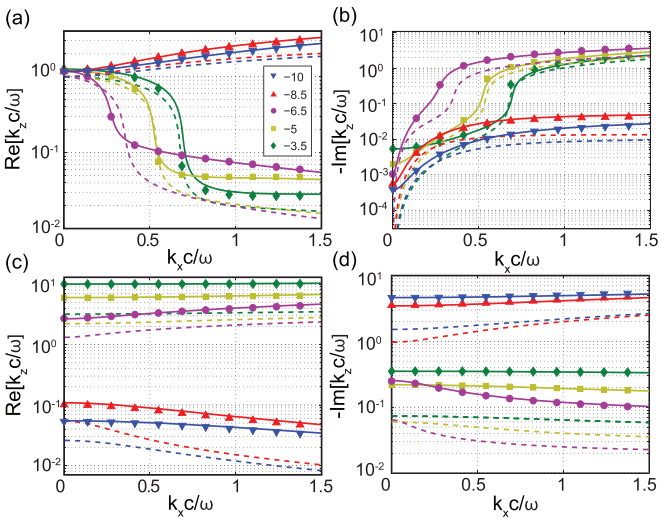


FIG. 7. (Color online) Dispersion of the modes guided by the nanowire metamaterial, calculated with full-wave solutions of Maxwell equations (symbols), the analytical technique presented in this work (solid lines), and with earlier approach, designed for highly conducting wires [33,34] (dashed lines); inset in (a) shows $\text{Re}[\epsilon_i]$; $\text{Im}[\epsilon_i] = -0.1; \epsilon_h = 1$.

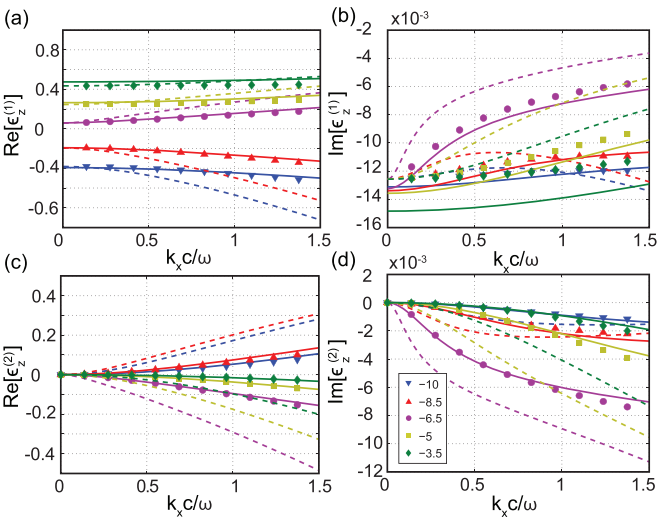


FIG. 9. (Color online) Effective permittivity [defined as $\epsilon_z = \langle \epsilon(x,y) E_z(x,y) \rangle / \langle E_z(x,y) \rangle$, see text] calculated with full-wave solutions of Maxwell equations (symbols), the analytical technique presented in this work (solid lines), and with earlier approach, designed for highly conducting wires [33,34] (dashed lines); note the difference in vertical scale between (a) and (c) and (b) and (d).

given by nontrivial solutions of the linear relationship

$$\widehat{\mathcal{H}_y}\alpha^- = (\widehat{\widehat{H^+}\widehat{S_{11}}} + \widehat{H^+}\widehat{S_{21}} + \widehat{H^-})\alpha^- = 0, \qquad \text{(B4)}$$

resulting in Eq. (5).

## APPENDIX C: COMPARISON WITH EARLIER NONLOCAL HOMOGENIZATION ATTEMPTS

As described in the paper, the problem of light interaction with nonlocal wire media has been considered before [24–35]. The majority of the studies that focus on high-frequency response of wire composites [24–31] predict a single extraordinary and a single ordinary wave at every frequency. The majority of studies that do predict existence of additional electromagnetic waves [32–35] have focused on optics for highly conductive (PEC-like) wires. References [33] and [34] present an attempt to generalize the developed formalism to the case of plasmonic media. Figures 7, 8, and 9 present a comparison of the formalism from Refs. [33] and [34], the approach described in this work, and full wave numerical solutions of Maxwell equations.

Figures 7 and 8 clearly demonstrate that, in contrast to the formalism presented in this work, the approach developed in Refs. [32–34] severely underestimates effective modal index of the waves propagating in plasmonic wire media (similar phenomenon can also be seen in Fig. 3 of Ref. [33]). This underestimation yields significant errors in calculations of optical properties of wire composites, seen in Fig. 5 of Ref. [34] that can be only be eliminated by using heuristic correction factor.

Finally, we note that our formalism not only adequately describes the effective modal index of light propagating in plasmonic wire media, but it also correctly predicts effective nonlocal permittivity of these modes. The latter fact is clearly seen in Fig. 9 (note that due to difference in vertical scale agreement for $\mathrm{Im}[\epsilon_z]$ looks worse than the agreement for $\mathrm{Re}[\epsilon_z]$).


[1] C. R. Simovski, P. A. Belov, A. V. Atrashchenko, and Y. S. Kivshar, Adv. Mater. **24**, 4229 (2012).
[2] J. Yao, Z. Liu, Y. Liu, Y. Wang, C. Sun, G. Bartal, A. M. Stacy, and X. Zhang, Science **321**, 930 (2008).
[3] Z. Jacob, I. I. Smolyaninov, and E. E. Narimanov, Appl. Phys. Lett. **100**, 161103 (2012).
[4] A. N. Poddubny, P. A. Belov, and Y. S. Kivshar, Phys. Rev. A **84**, 023807 (2011).
[5] O. Kidwai, S. V. Zhukovsky, and J. E. Sipe, Opt. Lett. **36**, 2530 (2011).
[6] W. Yan, M. Wubs, and N. A. Mortensen, Phys. Rev. B **86**, 205429 (2012).
[7] P. A. Belov, Y. Zhao, S. Tse, P. Ikonen, M. G. Silveirinha, C. R. Simovski, S. Tretyakov, Y. Hao, and C. Parini, Phys. Rev. B **77**, 193108 (2008).
[8] P. A. Belov, Y. Zhao, S. Sudhakaran, A. Alomainy, and Y. Hao, Appl. Phys. Lett. **89**, 262109 (2006).
[9] S. Thongrattanasiri and V. A. Podolskiy, Opt. Lett. **34**, 890 (2009).
[10] Z. Jacob, L. V. Alekseyev, and E. Narimanov, Opt. Express **14**, 8247 (2006).
[11] A. Salandrino and N. Engheta, Phys. Rev. B **74**, 075103 (2006).
[12] Z. Liu, H. Lee, Y. Xiong, C. Sun, and X. Zhang, Science **315**, 1686 (2007).
[13] A. V. Kabashin, P. Evans, S. Pastkovsky, W. Hendren, G. A. Wurtz, R. Atkinson, R. Pollard, V. A. Podolskiy, and A. V. Zayats, Nat. Mater. **8**, 867 (2009).
[14] L. S. Dolin, Izv. Vyssh. Uchebn. Zaved. Radiofiz. **4**, 964 (1961).
[15] J. B. Pendry, D. Schurig, and D. Smith, Science **312**, 1780 (2006).
[16] W. Cai, U. K. Chettiar, A. V. Kildishev, and V. M. Shalaev, Nat. Photon. **1**, 224 (2007).
[17] E. Narimanov, H. Li, Yu. A. Barnakov, T. U. Tumkur, and M. A. Noginov, arXiv:1109.5469.
[18] V. V. Yakovlev, W. Dickson, A. Murphy, J. McPhillips, R. M. Pollard, V. A. Podolskiy, and A. V. Zayats, Adv. Mater. **25**, 2351 (2013).
[19] G. A. Wurtz, R. Pollard, W. Hendren, G. P. Wiederrecht, D. J. Gosztola, V. A. Podolskiy, and A. V. Zayats, Nat. Nanotech. **6**, 107 (2011).
[20] R. W. Ziolkowski, Phys. Rev. E **70**, 046608 (2004).
[21] M. Silveirinha and N. Engheta, Phys. Rev. Lett. **97**, 157403 (2006).
[22] N. Engheta, Science **340**, 286 (2013).
[23] M. A. Noginov and V. A. Podolskiy, Eds., *Tutorials in Metamaterials* (CRC, Boca Raton, FL, 2012).
[24] S. P. Burgos, R. Waele, A. Polmam, and H. A. Atwater, Nat. Mater. **9**, 407 (2010).
[25] S. M. Prokes, Orest J. Glembocki, J. E. Livenere, T. U. Tumkur, J. K. Kitur, G. Zhu, B. Wells, V. A. Podolskiy, and M. A. Noginov, Opt. Express **21**, 14962 (2013).
[26] A. Murphy, Y. Sonnefraud, A. V. Krasavin, P. Ginzburg, F. Morgan, J. McPhillips, G. Wurtz, S. A. Maier, A. V. Zayats, and R. Pollard, Appl. Phys. Lett. **102**, 103103 (2013).
[27] A. K. Sarychev, R. C. McPhedran, and V. M. Shalaev, Phys. Rev. B **62**, 8531 (2000).
[28] R. Atkinson, W. R. Hendren, G. A. Wurtz, W. Dickson, A. V. Zayats, P. Evans, and R. J. Pollard, Phys. Rev. B **73**, 235402 (2006).
[29] J. Elser, R. Wangberg, V. A. Podolskiy, and E. E. Narimanov, Appl. Phys. Lett. **89**, 261102 (2006).
[30] G. A. Wurtz, W. Dickson, D. O'Connor, R. Atkinson, W. Hendren, P. Evans, R. Pollard, and A. V. Zayats, Opt. Express **16**, 7460 (2008).
[31] A. L. Pokrovsky and A. L. Efros, Phys. Rev. B **65**, 045110 (2002).
[32] P. A. Belov, R. Marques, S. I. Maslovski, I. S. Nefedov, M. Silveirinha, C. R. Simovski, and S. A. Tretyakov, Phys. Rev. B **67**, 113103 (2003).

[33] M. G. Silveirinha, Phys. Rev. E **73**, 046612 (2006).
[34] M. G. Silveirinhna, P. A. Belov, and C. R. Simovski, Phys. Rev. B **75**, 035108 (2007).
[35] R. J. Pollard, A. Murphy, W. R. Hendren, P. R. Evans, R. Atkinson, G. A. Wurtz, A. V. Zayats, and V. A. Podolskiy, Phys. Rev. Lett. **102**, 127405 (2009).
[36] See Supplemental Material at http://link.aps.org/supplemental/10.1103/PhysRevB.89.035111 for details of numerical solutions of Maxwell equations and supplemental numerical codes.
[37] J. C. M. Garnett, Philos. Trans. R. Soc. London B **203**, 385 (1904).
[38] S. I. Pekar, Sov. Phys. JETP **6**, 785 (1958).
[39] J. D. Jackson, *Classical Electrodynamics*, 3rd ed. (John Wiley and Sons, New York, 1999).
[40] A. Boardman, *Electromagnetic Surface Modes* (John Wiley and Sons, Sydney, 1982).
[41] S. M. Rytov, Sov. Phys. JETP, **2**, 466 (1956).
[42] P. Yeh, A. Yariv, and C.-S. Hong, J. Opt. Soc. Am. **67**, 423 (1977).
[43] E. Doron and U. Smilansky, Phys. Rev. Lett. **68**, 1255 (1992).
[44] O. A. Starykh, P. R. J. Jacquod, E. E. Narimanov, and A. D. Stone, Phys. Rev. E **62**, 2078 (2000).
[45] H. E. Tureci, H. G. L. Schwefel, P. Jacquod, and A. D. Stone, Progr. Optics, **47**, 75 (2005).